# Properties of a one-dimensional metallophotonic crystal

J. T. Shen[1,2,*] and P. M. Platzman[2]
[1]*Department of Electrical Engineering, Stanford University, Stanford, California 94305, USA*
[2]*Bell Laboratories, Lucent Technologies, Murray Hill, New Jersey 07974, USA*
(Received 11 March 2004; published 8 July 2004)

We analyze the structure of a periodic arrangement of optically thick metallic gratings that have very narrow slits. This structure permits perfect transmission of light in some frequency range and is analogous to a one-dimensional all-dielectric photonic crystal. Our study shows this structure has many unusual features due to evanescent modes. One of these is that its band diagram has flat bands at long wavelengths. Another feature is that this structure can enhance the fields locally. More significantly, we show that a manipulation of the positions of the slits on adjacent metal films produces lateral displacement along the grating surface for a transmitted beam of finite cross section. This shift is similar to the birefringence in crystal optics.

DOI: 10.1103/PhysRevB.70.035101 PACS number(s): 42.70.Qs, 41.20.Jb, 78.70.Gq, 84.40.−x

Photonic band gap (PBG) crystals have attracted great attention in recent years, and are still under intense theoretical and experimental investigations. These artificial crystals usually consist of carefully designed periodic modulation of dielectric materials in space, and consequently show band gaps centered on desired frequencies.[1,2] This feature makes the PBG crystal a potentially new material for photonic devices. However, these photonic devices are rarely made of metal. The obvious reason is that metals are always lossy, for all frequencies of interest.

There have been many attempts to incorporate metals into all-dielectric photonic crystals, both in theory[3–7] and in experiments.[8–11] All of these investigations concentrate on two-dimensional or three-dimensional metallodielectric structures in which the metal components are in the form of either mesh,[10] wire,[6] sphere,[3] or capacitors,[11] and are embedded in a dielectric matrix. These metal components can be interconnected, as in the mesh case; or disconnected, as in the wire, sphere, or capacitors cases. In one dimension, an all-dielectric PBG crystal consists of alternating high and low dielectric slabs with designed widths.[2] A direct analogy is to replace one kind of the dielectric materials with very thin metal films,[12] but the transmission is small.

Recently, several experiments have shown that the extraordinary optical transmission of light through 2-D perforated metallic films can be obtained at wavelengths up to 10 times larger than the diameter of the holes.[13–17] It has also been shown theoretically that similar extraordinary optical transmissions can also be found for metallic gratings with very narrow slits.[18–23] These discoveries open up a new way for light to be transmitted through metal foils.

In this paper, we give an almost analytic solution for the propagation of light through a periodic structure composed of metallic gratings with very narrow slits. We show the existence of a band structure, as well as many other interesting features of this metallic photonic crystal due to the evanescent modes between metal films.

Consider a stack of multilayer metal films in the vacuum with gratings, composed of slits, on each layer. In Fig. 1 we show a schematic view of the structures under study with the definition: the period of the grating ($d$), the width of the slit ($a$), the thickness of the metal films ($h$), the distance between two metal films ($s$) which determines the degree of coupling between evanescent modes, and the relative shift between the slits on adjacent films ($l$). Similar periodic multilayer grating systems consisting of all dielectric materials have been investigated using a curvilinear coordinate transformation and truncated transfer matrix.[24]

Following Refs. 18 and 25, we assume that the tangential electric field satisfies the surface-impedance boundary conditions.[26] This is true for a realistic metal with a large but negative dielectric constant $\epsilon$. In the slits, we know no matter how small, there are evanescent modes and a TEM mode which propagates. It is the TEM mode which dominates when the film is not too thin. Throughout this paper, we assume the incident electromagnetic wave is in $P$-polarization (i.e., the $H$ field is parallel to the slits), and retain only TEM mode in the slits. We analyze the structure consisting of perfect metal ($|\epsilon_{\text{metal}}|=\infty$) embedded in a medium with refraction index $n$. Hereafter $n$ is taken to be 1 for simplicity.

The magnetic fields on the $2j$-th film and in the region $2j+1$ (between the films) [see Fig. 1(a)] have a Bloch-wave type expression, respectively. The electric fields in each region are then obtained from Maxwell's equations. By matching the fields at each boundary, we can eliminate all the modes in region $2j+1$ and get an analytic form of the transfer matrix $T$ which connects the fields in the slits on adjacent films $2j$ and $2j+2$:

$$\begin{pmatrix} a_{2j+2} \\ b_{2j+2} \end{pmatrix} = \begin{pmatrix} \dfrac{(1+A)^2 u}{4B_-} - B_+ u & \dfrac{(1-A)(1+A)}{4B_-} + B_+ \\ \dfrac{(A-1)(A+1)}{4B_-} - B_+ & \dfrac{(1-A)(A-1)}{4B_- u} + \dfrac{B_+}{u} \end{pmatrix} \times \begin{pmatrix} a_{2j} \\ b_{2j} \end{pmatrix} \equiv T \begin{pmatrix} a_{2j} \\ b_{2j} \end{pmatrix}, \tag{1}$$

where $a_{2j}$ and $b_{2j}$ are the amplitudes of the forward and backward running magnetic fields for the TEM modes in the slits,

 

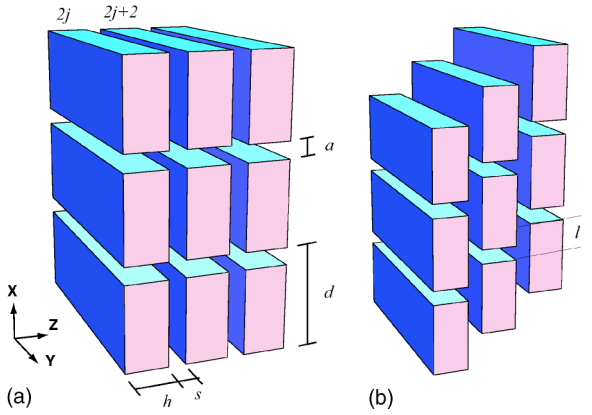


FIG. 1. (Color online) Schematics of the geometry. Shown in each graph is a 3-layer example. (a) The slits are perfectly aligned, $l=0$. (b) The slits are displaced by a distance $l$ relative to previous layers.

$$A \equiv \sum_{p=-\infty}^{\infty} \frac{w_p + w_p^{-1}}{w_p - w_p^{-1}} \frac{fkg_p^2}{\alpha_p},\ B_- \equiv \sum_{p=-\infty}^{\infty} \frac{e^{-iG_p l}}{w_p - w_p^{-1}} \frac{fkg_p^2}{\alpha_p},$$

$$B_+ \equiv \sum_{p=-\infty}^{\infty} \frac{e^{+iG_p l}}{w_p - w_p^{-1}} \frac{fkg_p^2}{\alpha_p}, \tag{2}$$

$k$ is the momentum of incident light in the medium, $G_p = k_x + 2\pi p/d$ is the parallel momentum along the metal surface of the $p$-th diffraction order, $\alpha_p \equiv \sqrt{k^2 - G_p^2}$ is the momentum in the $z$-direction, $f \equiv a/d$ is the area filling factor of the slits, $w_p \equiv e^{i\alpha_p s}$ is the phase accumulation across the distance $s$ between metal films, $u \equiv e^{ikh}$ is the phase accumulation across each slit waveguide, and $g_p \equiv \mathrm{sinc}(G_p a/2)$. When $\alpha_p$ is imaginary, the $p$-th diffraction mode is evanescent. By examining the eigenvalues of the transfer matrix $T$, we can determine the relation between $\omega$ and $k_x$ for which there is propagation through the slits.

For a finite number of layers, two more equations are needed in order to compute the transmission and reflection amplitudes. These two equations are

$$(a_2 + b_2 u) = 2g_0 - \phi(a_2 - b_2 u),$$

$$(a_{2n} u + b_{2n}) = \phi(a_{2n} u - b_{2n}). \tag{3}$$

Here

$$\phi = \sum_{p=-\infty}^{\infty} \frac{fkg_p^2}{\alpha_p}. \tag{4}$$

The transmission and reflection amplitudes for the $p$-th diffraction order are then given by

$$t_p = f\frac{kg_p}{\alpha_p}(a_{2n} u - b_{2n}) e^{-iG_p(n-1)l},$$

$$r_p = \delta_{0,p} - f\frac{kg_p}{\alpha_p}(a_2 - b_2 u). \tag{5}$$

The details of the derivation are presented in the Appendix.

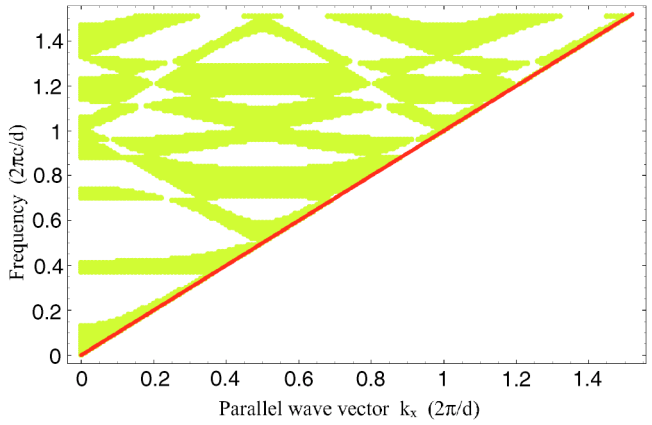


FIG. 2. (Color online) Band structure of infinite multilayered metal gratings with narrow slits perfectly aligned. The shaded area corresponds to passing bands, and white regions to stop gaps. The thick line indicates the light cone. $a=\frac{1}{7}$, $d=1$, $h=\frac{8}{7}$, and $s=\frac{4}{7}$. $d$, the lattice constant on the film, is the length unit.

Assume the slits are perfectly aligned (i.e., $l=0$). Considering an incoming plane wave with momentum $k_x$ along the metal surface, Fig. 2 shows the projected band diagram for a specific set of dimensionless parameters: $a=\frac{1}{7}$, $d=1$, $h=\frac{8}{7}$, and $s=\frac{4}{7}$, where $d$ is adopted as a length unit throughout this paper. In the diagram, we see a low frequency propagating band as well as two very flat bands developed at normalized frequency $\omega=0.37$ and 0.7. For a given frequency, the flatness of these bands means there is propagation of waves for a wide range of incident angles. It also implies standing waves along the plane of metal films, since $\partial\omega/\partial k_x \to 0$. These flat bands are reminiscent of the flat bands from the poles of the transmission coefficient for only one grating metal film.[18,27] Figure 3 shows the dispersion relation between the Bloch wave vector $K$ in the $z$-direction and the frequency $\omega$. At low frequency, the dispersion is linear. Figures 4(b) and 4(c) show the zeroth-order transmittance for four metal films with different $s$. Compared to single layer case, new peaks emerge at long wavelength and evolve into

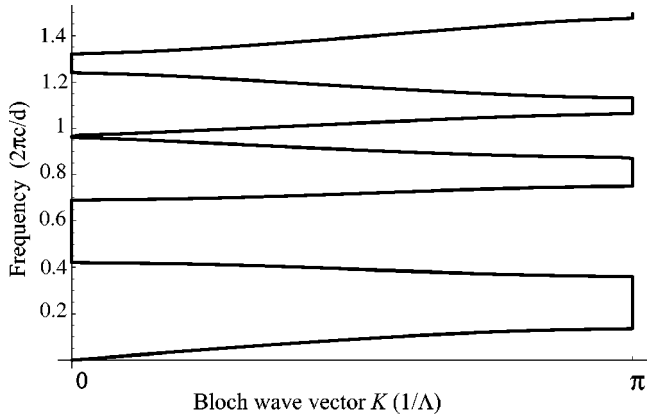


FIG. 3. The dispersion relation between $K$ and $\omega$ when $l=0$. The Bloch wave vector $K$ is in units of $\Lambda \equiv h+s$, the frequency $\omega$ is in units of $2\pi c/d$, i.e., $K$=Block wave vector$\times\Lambda$, $\omega = d/\lambda$. $a=1/7$, $d=1$, $h=8/7$, $s=4/7$, and $l=0$.

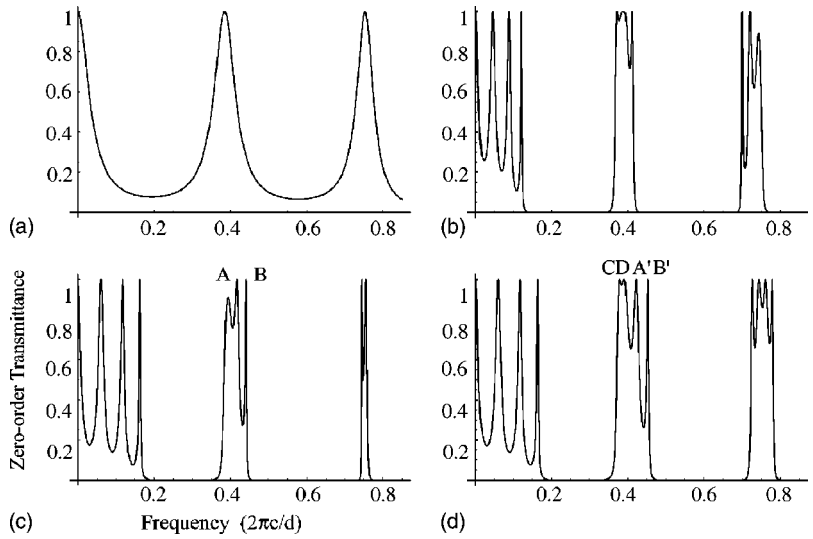


FIG. 4. Zeroth-order transmittance curves for normally incident light. $a=\frac{1}{7}$, $d=1$, and $h=\frac{8}{7}$. (a) Single layer. (b), (c), (d) Four layers. (b) $s=\frac{4}{7}$, $l=0$. (c) $s=\frac{2}{7}$, $l=0$. (d) $s=\frac{2}{7}$, $l=0.3$. Capital letters label the transmittance peaks.

the lowest propagating bands. The range of these peaks is widened when $s$ decreases, due to a stronger interaction between evanescent modes. Changing the value of $s$ also has a nontrivial effect on higher bands.

It is easy to show that $|a_{2n}u-b_{2n}|$ is the electric field strength at the exit of the slits on the last layer of metal film. For normal incidence, $g_0=1$, $\alpha_0=k$, so the existence of perfect transmission implies $|a_{2n}u-b_{2n}|=1/f$ when the frequency is within the propagating bands. That is, there is strong field enhancement associated with the perfect transmission, and the degree of amplitude enhancement is exactly inversely proportional to the area ratio (filling fraction) $f$ of the slits. This strong field consists of largely evanescent with a small amount of propagating waves. The feature of strong field enhancement is desired in nonlinear optics. In Fig. 5 we show the contour plot for the intensity of electric field for two metal films at the first band with the resonance frequency $\omega=0.388$, and at lowest band with the resonance frequency $\omega=0.089$, respectively. There is a node (i.e., intensity is zero) in the slits when the frequency is in the first flat band; while the slits are all lit up when the frequency is in the lowest band. As to the phase of the electric field, at the first band with the resonance frequency $\omega=0.388$, the electric fields on both sides of the same metal film are pointing in the opposite directions, and are pointing in the same direction on adjacent films, as indicated by the arrows in Fig. 5(a); while for the lowest band in Fig. 5(b), the electric fields are pointing in the same direction on both sides of the same film, and are pointing in the opposite directions on adjacent films. This phase relation is closely connected with the number of nodes in the slits, and is common for one-dimensional systems.

When the slits on adjacent films are not aligned ($l\neq 0$), the phase $\varphi(l,k_x)$ of the transmission coefficient $t_p$ gains an additional amount from the relative shift $l$. This additional amount has contributions explicitly from the exponent $G_p l$ in Eq. (5) for each layer and implicitly from $a_{2n}$ and $b_{2n}$. This change in $\varphi(l,k_x)$ has interesting consequences.

For a light beam with a finite cross section incident on a thin film, the transmitted beam is displaced along the surface at the $x$-direction by an amount of $d_x=(\partial\varphi(l,k_x)/\partial k_x)_{k_{x0}}$, if the incident beam has $k_x$ sharply peaked at $k_{x0}$. For the system in question, when the slits are perfectly aligned ($l=0$), $d_x$ is 0 for a normally incident light beam ($k_{x0}=0$); while when $l\neq 0$, $d_x$ is not 0 for normally incident light beam, i.e., the transmitted beam is displaced by an amount of $d_x$. This is analogous to the extraordinary beam of the birefringence in crystal optics. In Fig. 6, we show $d_x$ as a function of $k_x$. When $\omega=0.3785$, the displacement $d_x$ is roughly 1.68 (or $1.68\times d/2\pi$ in dimensional units). $d_x$ can accumulate and is numerically linearly proportional to the number of layers, as

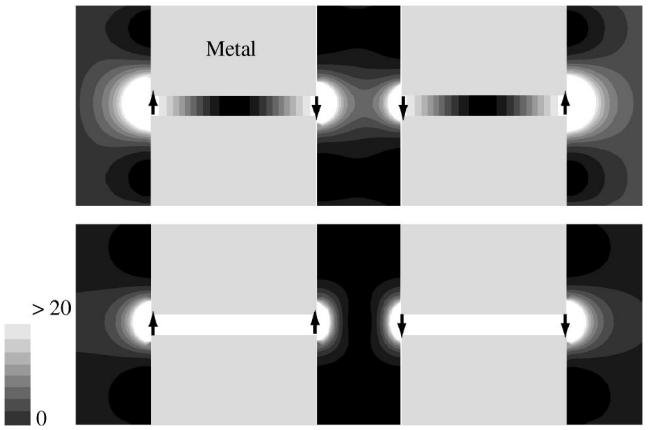


FIG. 5. Contour plot of the intensity of electric fields for normally incident light for two layers of metal films (shown as gray shaded regions). The electric field amplitude of the incident light is 1. (a) at the resonance frequency $\omega=0.388$ (the first flat band). (b) at the resonance frequency $\omega=0.089$ (the lowest band). The strong field enhancement in the proximity of the entrance and exit of the slits are clearly seen. $a=\frac{1}{7}$, $d=1$, $h=\frac{8}{7}$, and $s=\frac{4}{7}$. The amplitude enhancement factor is $1/f=d/a=7$. The arrows indicate the orientations of the electric fields at each location.

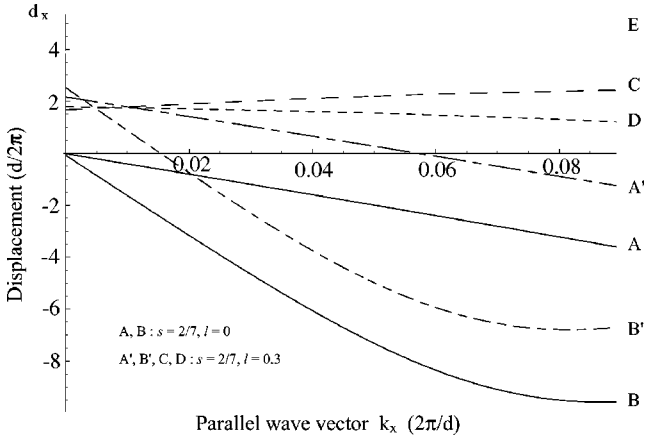


FIG. 6. Lateral displacement $d_x$ as a function of $k_x$ for four layers of metal films. The capital letter by each curve indicates the corresponding transmittance peak in Fig. 4. The gray curve $E$ has the same parameters as curve $C$ but with 8 layers, instead of 4 layers. Peaks $A$ and $A'$, $B$ and $B'$, $C$, and $D$ have similar behaviors, respectively.

shown by the curves $(C)$ and $(E)$ in Fig. 6. $d_x$ gets larger when $s$ is decreased.

A pictorial way of saying this is that the incident light makes turns in between the metal films and is displaced by the ladder-type structure, layer by layer, when it comes out on the other side. This is in contrast to passing through a simple dielectric layer of the same thickness, where an incident beam is not laterally shifted at normal incidence, and is shifted negatively only when the beam is incident at an angle. The physics is governed by both the propagating modes as well as the evanescent modes. In between the metal films, although the fields at the openings of the slits consist of both modes, most contributions are from the evanescent modes. This has the effect of changing the quasi-resonant frequencies in the slits where the propagating modes dominate, and can be described phenomenologically by the "effective impedance match" method. Furthermore, the fields at the openings of the slits can couple to each other, as can be clearly seen from Figs. 4(c) and 4(d): the peaks below $\omega = 0.2$ [the lowest band, the field profile is pictured at Fig. 5(b)] are insensitive to the misalignment, while the first band around $\omega = 0.4$ has qualitative changes [the field profile is pictured in Fig. 5(a)]. The coupling is largely determined by the profiles of the fields at the openings.

At a frequency range in which the magnitude of the dielectric constant of the metal is not infinite but complex, the analytic results for the aligned case still can be obtained via the corresponding changes in Eqs. (2) and (3):

$$A \to \sum_{p=-\infty}^{\infty} \frac{\left(1-\frac{k}{\alpha_p}\eta\right)w_p + \left(1+\frac{k}{\alpha_p}\eta\right)w_p^{-1}}{\left(1-\frac{k}{\alpha_p}\eta\right)^2 w_p - \left(1+\frac{k}{\alpha_p}\eta\right)^2 w_p^{-1}} \frac{fkg_p^2}{\alpha_p},$$

$$B_+, B_- \to \sum_{p=-\infty}^{\infty} \frac{1}{\left(1-\frac{k}{\alpha_p}\eta\right)^2 w_p - \left(1+\frac{k}{\alpha_p}\eta\right)^2 w_p^{-1}} \frac{fkg_p^2}{\alpha_p},$$

$$(a_2 + b_2 u) = 2\frac{\alpha_0}{\alpha_0 + k\eta} g_0 - \phi(a_2 - b_2 u),$$

$$(a_{2n} u + b_{2n}) = \phi(a_{2n} u - b_{2n}), \tag{6}$$

where $\phi$ now is

$$\phi = \sum_{p=-\infty}^{\infty} \frac{fkg_p^2}{\alpha_p + k\eta}, \tag{7}$$

and $\eta = \varepsilon_{\text{metal}}^{-1/2}$ is a small complex number. The above formula is accurate up to the order of $\eta^2$. For microwave frequency, this effect is completely negligible. For visible light, at resonance frequencies, since the fields largely localize around the slits, the attenuation of the em wave is also not so appreciable. At $\lambda = 1.5$ $\mu$m for five layers metal films of gold, the maximum transmission can be as large as 90%, this allows many practical applications.

In conclusion, we have shown the existence of projected band structure of the multilayer structure of metal gratings, the possibility to locally enhance the em fields, as well as the lateral displacement of normally incident beams and the role played by evanescent modes.

## ACKNOWLEDGMENTS

J.T. Shen wishes to acknowledge the interesting discussions with Professor Joannopoulos, Professor Schultz, E. Lidorikis, D. Roundy, Ho-Bun Chan, M. Ibanescu, and C. Luo.

## APPENDIX A: DERIVATION OF THE TRANSFER MATRIX *T*

In this appendix, we give the details of the derivation for the transfer matrix $T$ in Eq. (1), as well as for the case when loss in the metal is present. The symmetry properties of the transfer matrix is discussed in Appendix B.

### 1. Transfer matrix without loss

The magnetic fields on the $2j$-th region in the slits ($j$-th film) and in the region $2j+1$ (between the films) [see Fig. 1(a)] can be written in the following forms: In region $2j$:

$$H_y(x,z) = a_{2j}^m e^{ik[z-(j-1)(s+h)]} + b_{2j}^m e^{-ik[z-(j-1)(s+h)-h]}, \quad \text{in the } m\text{-th slit}, \tag{A1}$$

$$E_x(x,z) = \begin{cases} a_{2j}^m e^{ik[z-(j-1)(s+h)]} - b_{2j}^m e^{-ik[z-(j-1)(s+h)-h]}, & \text{if in the } m\text{-th slit}, \\ 0, & \text{otherwise}. \end{cases} \quad \text{(A2)}$$

In region $2j+1$:

$$H_y(x,z) = \sum_{p=-\infty}^{\infty} (u_{p,2j+1} e^{i\alpha_p[z-(j-1)(s+h)-h]} + v_{p,2j+1} e^{-i\alpha_p[z-(j-1)(s+h)-h]}) e^{iG_p x}, \quad \text{(A3)}$$

$$E_x(x,z) = \sum_{p=-\infty}^{\infty} \frac{\alpha_p}{k} (u_{p,2j+1} e^{i\alpha_p[z-(j-1)(s+h)-h]} - v_{p,2j+1} e^{-i\alpha_p[z-(j-1)(s+h)-h]}) e^{iG_p x}; \quad \text{(A4)}$$

$k$ is the momentum of incident light in the medium, $G_p = k_x + 2\pi p/d$ is the parallel momentum along the metal surface of the $p$-th diffraction order, $\alpha_p \equiv \sqrt{k^2 - G_p^2}$ is the momentum in the $z$-direction, $a_{2j}^m$ and $b_{2j}^m$ are the amplitudes of the forward and backward going waves in the $m$-th slit on the $2j$ region ($j$-th film), $m$ is an integer ranging from $-\infty$ to $\infty$ to label the slits on the $j$-th film (not an exponent). When the slits on the first film are labeled, all the slits on the subsequent films are also uniquely determined, since for each slit, there is one and only one slit on the next film which is within a $d/2$ vertical distance. The above choice of the relative phases between $a_{2j}^m$ and $b_{2j}^m$, and between $u_{p,2j+1}$ and $v_{p,2j+1}$ simplifies the final expression and does not change any physics.

The electric fields in each region are obtained from Maxwell's equation:

$$\nabla \times \mathbf{H} = \frac{1}{c}\frac{\partial \mathbf{E}}{\partial t} = -ik\mathbf{E}.$$

In our case, $\mathbf{H} = (0, H_y, 0)$ so $-ik\mathbf{E} = (-\partial_z H_y, 0, \partial_x H_y)$, and we get

$$ikE_x = \partial_z H_y,$$

$$ikE_z = -\partial_x H_y,$$

where the time dependence $e^{iwt}$is assumed.

Next is to match the boundary condition. The following condition is *sufficient* to determine the fields completely: The continuity of $E_x$ for all $x$, and the continuity of $H_y$ over the slits only.

(1) At $z=(j-1)(s+h)+h$ (the left boundary of the $2j$-th region, i.e., the $j$-th film):

(a) From the continuity of $H_y$ over the $m$-th slit $(md+(j-1)l-a/2) \leqslant x \leqslant (md+(j-1)l+a/2)$, we get

$$\sum_p (u_{p,2j+1} + v_{p,2j+1}) e^{iG_p x} = (a_{2j}^m + b_{2j}^m). \quad \text{(A5)}$$

(b) From the continuity of $E_x$:

$$\sum_p \frac{\alpha_p}{k}(u_{p,2j+1} - v_{p,2j+1}) e^{iG_p x} = \sum_m (a_{2j}^m u - b_{2j}^m) \times \theta\left(\left(md + (j-1)l + \frac{a}{2}\right) - x\right) \times \theta\left(x - \left(md + (j-1)l - \frac{a}{2}\right)\right). \quad \text{(A6)}$$

Integrate both sides of Eq. (A5) over the $m$-th slit, and use

$$\frac{1}{a}\int_{md+(j-1)l-a/2}^{md+(j-1)l+a/2} e^{iG_p x} dx = e^{iG_p(md+(j-1)l)} \frac{\sin(G_p a/2)}{G_p a/2} \equiv e^{iG_p(md+(j-1)l)} g_p;$$

we get

$$\sum_p (u_{p,2j+1} + v_{p,2j+1}) g_p e^{i(md+(j-1)l)} = a_{2j}^m u + b_{2j}^m. \quad \text{(A7)}$$

Multiply both sides of Eq. (A6) by $e^{-iG_{p'}x}$ amd integrate over a period:

$\frac{1}{d}\int_{md+(j-1)l-d/2}^{md+(j-1)l+d/2} (\cdot) dx$, where $(\cdot)$ denotes either side of Eq. (A6);

we get

$$\frac{\alpha_p}{k}(u_{p,2j+1} - v_{p,2j+1}) = (a_{2j}^m u - b_{2j}^m) f e^{-iG_p(md+(j-1)l)} g_p; \quad \text{(A8)}$$

$f \equiv a/d$ is the area filling factor of the slits.

(2) At $z=j(s+h)$ (the right boundary of the $2j$-th region, i.e., the $j$-th film):

(a) From $H_y$:

$$\sum_p (u_{p,2j+1} e^{i\alpha_p s} + v_{p,2j+1} e^{-i\alpha_p s}) e^{iG_p x} = (a_{2j+2}^m + b_{2j+2}^m u). \quad \text{(A9)}$$

(b) From $E_x$

$$\sum_p \frac{\alpha_p}{k}(u_{p,2j+1} e^{i\alpha_p s} - v_{p,2j+1} e^{-i\alpha_p s}) e^{iG_p x} = \sum_m (a_{2j+2}^m - b_{2j+2}^m u) \times \theta\left(\left(md + jl + \frac{a}{2}\right) - x\right) \times \theta\left(x - \left(md + jl - \frac{a}{2}\right)\right). \quad \text{(A10)}$$

Integrate over the corresponding slit $(md+jl-a/2) \leqslant x \leqslant (md+jl+a/2)$ and period $(md+jl-d/2) \leqslant x \leqslant (md+jl+d/2)$, respectively; as previousy, we get

$$\sum_p (u_{p,2j+1}w_p + v_{p,2j+1}w_p^{-1})g_p e^{i(md+jl)} = a_{2j+2}^m + b_{2j+2}^m u, \tag{A11}$$

$$\frac{\alpha_p}{k}(u_{p,2j+1}w_p - v_{p,2j+1}w_p^{-1}) = (a_{2j+2}^m - b_{2j+2}^m u) f e^{-iG_p(md+jl)} g_p. \tag{A12}$$

Therefore, from the Maxwell's equations and the boundary conditions, we obtain the following set of equations:

$$\sum_p (u_{p,2j+1} + v_{p,2j+1})g_p e^{i(md+(j-1)l)} = a_{2j}^m u + b_{2j}^m, \tag{A13}$$

$$\sum_p (u_{p,2j+1}w_p + v_{p,2j+1}w_p^{-1})g_p e^{i(md+jl)} = a_{2j+2}^m + b_{2j+2}^m u, \tag{A14}$$

$$\frac{\alpha_p}{k}(u_{p,2j+1} - v_{p,2j+1}) = (a_{2j}^m u - b_{2j}^m) f e^{-iG_p(md+(j-1)l)} g_p, \tag{A15}$$

$$\frac{\alpha_p}{k}(u_{p,2j+1}w_p - v_{p,2j+1}w_p^{-1}) = (a_{2j+2}^m - b_{2j+2}^m u) f e^{-iG_p(md+jl)} g_p. \tag{A16}$$

The intermediate variables $u_{p,2j+1}$ and $v_{p,2j+1}$ can be eliminated from the set of equations to get the transfer matrix between $a_{2j}^m$, $b_{2j}^m$, $a_{2j+2}^m$, and $b_{2j+2}^m$:

$$\begin{pmatrix} a_{2j+2}^m \\ b_{2j+2}^m \end{pmatrix} = \begin{pmatrix} \frac{(1+A)^2 u}{4B_-} - B_+ u & \frac{(1-A)(1+A)}{4B_-} + B_+ \\ \frac{(A-1)(A+1)}{4B_-} - B_+ & \frac{(1-A)(A-1)}{4B_- u} + \frac{B_+}{u} \end{pmatrix} \times \begin{pmatrix} a_{2j}^m \\ b_{2j}^m \end{pmatrix}, \tag{A17}$$

where

$$A \equiv \sum_{p=-\infty}^{\infty} \frac{w_p + w_p^{-1}}{w_p - w_p^{-1}} \frac{f k g_p^2}{\alpha_p},\ B_- \equiv \sum_{p=-\infty}^{\infty} \frac{e^{-iG_p l}}{w_p - w_p^{-1}} \frac{f k g_p^2}{\alpha_p},$$

$$B_+ \equiv \sum_{p=-\infty}^{\infty} \frac{e^{+iG_p l}}{w_p - w_p^{-1}} \frac{f k g_p^2}{\alpha_p}. \tag{A18}$$

The transmitted fields can be written as

$$H_y = \sum_p t_p e^{i\alpha_p[z-(n-1)(s+h)-h]} e^{iG_p x}, \tag{A19}$$

$$E_x = \sum_p \frac{\alpha_p}{k} t_p e^{i\alpha_p[z-(n-1)(s+h)-h]} e^{iG_p x}; \tag{A20}$$

$n$ is the total number of the metal films. Note the choice of phase already take into account of the total thickness of the system.

At $z=(n-1)(s+h)+h$ i.e., the right-most boundary, after integration over the corresponding slit and period, Eq. (A20) gives

$$t_p = f g_p \frac{k}{\alpha_p}(a_{2n}^m u - b_{2n}^m) e^{-iG_p(md+(n-1)l)}, \tag{A21}$$

while Eq. (A19) gives

$$(a_{2n}^m u + b_{2n}^m) = \sum_p t_p g_p e^{iG_p(md+(n-1)l)}. \tag{A22}$$

In Eq. (A21), on the left hand side, $t_p$, is independent of the slit label $m$; we now show the expression on the right hand side is also independent of $m$ too:

$$e^{-iG_p md} = e^{-ik_x md - i2\pi m} = e^{-ik_x md}.$$

When the incident wave comes in at an angle such that $k_x \neq 0$, the $m$-th slit gets an additional phase $e^{+ik_x md}$. This phase cancels the above one so the right hand side of Eq. (A21) is indeed independent of $m$, as it should be.

Substitute Eq. (A21) into Eq. (A22), we get

$$(a_{2n}^m u + b_{2n}^m) = (a_{2n}^m u - b_{2n}^m) \sum_p f g_p^2 \frac{k}{\alpha_p} \equiv (a_{2n}^m u - b_{2n}^m)\phi, \tag{A23}$$

which is one of Eq. (3).

The total fields on the incident side can be written as

$$H_y(x,z) = \sum_p (\delta_{0,p} e^{i\alpha_p z} + r_p e^{-i\alpha_p z}) e^{iG_p x}, \tag{A24}$$

$$E_x(x,z) = \sum_p \frac{\alpha_p}{k}(\delta_{0,p} e^{i\alpha_p z} - r_p e^{-i\alpha_p z}) e^{iG_p x}. \tag{A25}$$

Matching the boundary conditions at $z=0$, we get

$$\sum_p g_p(\delta_{0,p} + r_p) e^{iG_p md} = a_2^m + b_2^m u, \tag{A26}$$

$$\frac{\alpha_p}{k}(\delta_{0,p} - r_p) = f g_p (a_2^m - b_2^m u) e^{-iG_p md}. \tag{A27}$$

From Eq. (A27),

$$r_p = \delta_{0,p} - \frac{k}{\alpha_p} f g_p (a_2^m - b_2^m u) e^{-iG_p md}. \tag{A28}$$

Plug into Eq. (A26), we get

$$a_2^m + b_2^m u = 2g_0 - \phi(a_2^m - b_2^m u); \tag{A29}$$

Eqs. (A29) and (A23) serve as the "boundary counditions" of the transfer matrix, Eq. (A17), for $a_{2j}^m$ and $b_{2j}^m$.

From the expression of the fields in the slits, Eq. (A1), at $z=(n-1)(s+h)+h$, the interface between the last film and the transmitted region:

$$E_x(x, z = (n-1)(s+h)+h) = a_{2n}^m u - b_{2n}^m.$$

From the expression of the transmission coefficient of $p$-th order:

$$|t_p| = \left| f g_p \frac{k}{\alpha_p} (a_{2n}^m u - b_{2n}^m) e^{-iG_p(md+(n-1)l)} \right| = \left| f g_p \frac{k}{\alpha_p} (a_{2n}^m u - b_{2n}^m) \right|. \quad \text{(A30)}$$

At perfect transmission, the absolute value of zeroth-order transmission coefficient, $|t_0|$, is 1, i.e., $|a_{2n}^m u - b_{2n}^m| = 1/f$, since $g_0 = k/\alpha_0 = 1$. This means the amplitude of the electric field is amplified by factor $1/f$ (the amplitude of incoming wave is 1), which is larger than the $\sqrt{1/f}$ result given by energy conservation consideration at the far field. The field amplification relation holds even when $l \neq 0$.

### 2. Transfer matrix with loss

For real metals, there is always loss present. When the magnitude of the dielectric constant of metal, $|\epsilon_{\text{metal}}|$, is large, we can obtain the transfer matrix by perturbation.

At the boundary of a vacuum and a metal, the fields immediately *external* to the metal surface obeys the following "boundary impedance conditions:"[26]

$$\mathbf{E}_t = \eta \hat{\mathbf{n}} \times \mathbf{H}_t, \quad \text{(A31)}$$

where $\mathbf{E}_t$ and $\mathbf{H}_t$ are the tangential components of electric and magnetic fields at the metal surface; $\hat{\mathbf{n}}$ is the unit normal vector on the boundary pointing in the vacuum direction; $\eta \equiv \epsilon_{\text{metal}}^{-1/2}$ is the surface impedance, its real and imaginary parts define the dissipated energy and the phase shift of the reflected electromagnetic wave, respectively.

For our case, $\mathbf{E}_t = E_x \hat{\mathbf{x}}$, and $\mathbf{H}_t = H_y \hat{\mathbf{y}}$. Here we outline the derivation of the case when $l=0$. By requiring $E_x$ and $H_y$ to be continuous over the slits, and $E_x$ to obey the boundary impedance condition, we obtain the following set of equations, after the integration:

$$\frac{\alpha_p}{k}(\delta_{0,p} - r_p) = f g_p (a_2 - b_2 u) + \eta(\delta_{0,p} + r_p),$$

$$\sum_p g_p (\delta_{0,p} + r_p) = a_2 + b_2 u,$$

$$\frac{\alpha_p}{k}(u_{p,3} - v_{p,3}) = f g_p (a_2 u - b_2) - \eta(u_{p,3} + v_{p,3}),$$

$$\sum_p g_p (u_{p,3} + v_{p,3}) = a_2 u + b_2,$$

$$\frac{\alpha_p}{k}(u_{p,3} w_p - v_{p,3} w_p^{-1}) = f g_p (a_4 - b_4 u) + \eta(u_{p,3} w_p + v_{p,3} w_p^{-1}),$$

$$\sum_p g_p (u_{p,3} w_p + v_{p,3} w_p^{-1}) = a_4 + b_4 u,$$

$$\vdots$$

$$\frac{\alpha_p}{k} t_p = f g_p (a_{2n} u - b_{2n}) - \eta t_p,$$

$$\sum_p g_p t_p = a_{2n} u + b_{2n}. \quad \text{(A32)}$$

Eliminating the intermediate variables $u_{p,2j+1}$ and $v_{p,2j+1}$, we obtain

$$\begin{pmatrix} a_{2j+2} \\ b_{2j+2} \end{pmatrix} = \begin{pmatrix} \frac{(1+A)^2 u}{4B_-} - B_+ u & \frac{(1-A)(1+A)}{4B_-} + B_+ \\ \frac{(A-1)(A+1)}{4B_-} - B_+ & \frac{(1-A)(A-1)}{4B_- u} + \frac{B_+}{u} \end{pmatrix} \times \begin{pmatrix} a_{2j} \\ b_{2j} \end{pmatrix}, \quad \text{(A33)}$$

where

$$A = \sum_{p=-\infty}^{\infty} \frac{\left(1 - \frac{k}{\alpha_p}\eta\right) w_p + \left(1 + \frac{k}{\alpha_p}\eta\right) w_p^{-1}}{\left(1 - \frac{k}{\alpha_p}\eta\right)^2 w_p - \left(1 + \frac{k}{\alpha_p}\eta\right)^2 w_p^{-1}} \frac{f k g_p^2}{\alpha_p},$$

$$B_+ = B_- = \sum_{p=-\infty}^{\infty} \frac{1}{\left(1 - \frac{k}{\alpha_p}\eta\right)^2 w_p - \left(1 + \frac{k}{\alpha_p}\eta\right)^2 w_p^{-1}} \frac{f k g_p^2}{\alpha_p},$$

with the "boundary conditions"

$$(a_2 + b_2 u) = 2\frac{\alpha_0}{\alpha_0 + k\eta} g_0 - \phi(a_2 - b_2 u),$$

$$(a_{2n} u + b_{2n}) = \phi(a_{2n} u - b_{2n}), \quad \text{(A34)}$$

where $\phi$ now is

$$\phi = \sum_{p=-\infty}^{\infty} \frac{f k g_p^2}{\alpha_p + k\eta}. \quad \text{(A35)}$$

The transmission and reflection amplitudes are

$$t_p = f \frac{k g_p}{\alpha_p + k\eta}(a_{2n} u - b_{2n}),$$

$$r_p = \frac{\alpha_p - k\eta}{\alpha_p + k\eta}\delta_{0,p} - f \frac{k g_p}{\alpha_p + k\eta}(a_2 - b_2 u).$$

## APPENDIX B: SYMMETRY PROPERTIES OF THE TRANSFER MATRIX *T*

The transfer matrix $T$ in Eq. (1) has the following properties.

(1) A is always pure imaginary for all values of parameters, i.e., $A^* = -A$.

(2) When the slits on all metal films are perfectly aligned, i.e., $l=0$, we have $B_+ = B_-$; when the slits are displaced by a distance $l$ relative to previous layers, i.e., $l \neq 0$, we have $B_+^* = -B_-$. Let $B_+ = x + iy$; then $B_- = -x + iy$, i.e., $B_+ = B_- e^{i\theta}$ and $|B_+/B_-| = 1$. When $k_x = 0$, $\theta$ is a periodic function with period $d$.

(3) The determinant of the transfer matrix has magnitude 1: $\det T = B_+/B_- = e^{i\theta} \Rightarrow |\det T| = 1$.

(4) The relation between the diagonal elements of $T$:

$$T_{11}^* = \frac{(1+A^*)^2 u^*}{4B_-^*} - B_+^* u^* = \frac{(1-A)^2}{4(-B_+)u} + \frac{B_-}{u}$$
$$= \frac{(1-A)(A-1)}{4B_+ u} + \frac{B_-}{u} = \left( \frac{(1-A)(A-1)}{4B_- u} + \frac{B_+}{u} \right) e^{-i\theta}$$
$$= T_{22} e^{-i\theta}.$$

(5) It is also straightforward to show that $T_{12} = T_{21} e^{i\theta}$.

Therefore, the transfer matrix has the following general form:

$$\begin{pmatrix} T_{11} & T_{21}^* e^{i\theta} \\ T_{21} & T_{11}^* e^{i\theta} \end{pmatrix},$$

which is also as the same form of the transfer matrix of a system obeying energy conservation but not time reversal symmetry. Note that this property is not changed for a different choice of the relative phase between $a_{2j}$ and $b_{2j}$. It is clear that the nonzero slit displacement $l$ breaks the parity symmetry with respect to the $z$-axis. The time-reversal invariance is restored when the transformation is accompanied by $l \rightarrow -l$ at the same time.

*Electronic address: jushen@stanford.edu


[1] E. Yablonovitch, Phys. Rev. Lett. **58**, 2059 (1987).

[2] J. D. Joannopoulos, R. D. Mead, and J. N. Winn, *Photonic Crystal* (Princeton University Press, Princeton, NJ, 1995).

[3] A. R. McGurn and A. A. Maradudin, Phys. Rev. B **48**, 17576 (1993).

[4] J. B. Pendry, J. Mod. Opt. **41**, 109 (1994).

[5] M. M. Sigalas, C. T. Chan, K. M. Ho, and C. M. Soukoulis, Phys. Rev. B **52**, 11744 (1995).

[6] J. B. Pendry, A. J. Holden, W. J. Stewart, and I. Youngs, Phys. Rev. Lett. **76**, 4773 (1996).

[7] S. Fan, P. R. Villeneuve, and J. D. Joannopoulos, Phys. Rev. B **54**, 11245 (1996).

[8] D. R. Smith, S. Schultz, N. Kroll, M. Sigalas, K. M. Ho, and C. M. Soukoulis, Appl. Phys. Lett. **65**, 645 (1994).

[9] E. R. Brown and O. B. McMahon, Appl. Phys. Lett. **67**, 2138 (1995).

[10] D. F. Sieveniper, M. E. Sickmiller, and E. Yablonovitch, Phys. Rev. Lett. **76**, 2480 (1996).

[11] D. F. Sievenpiper, E. Yablonovitch, J. N. Winn, S. Fan, P. R. Villeneuve, and J. D. Joannopoulos, Phys. Rev. Lett. **80**, 2829 (1997).

[12] M. Scalora, M. J. Bloemer, A. S. Pethel, J. P. Dowling, C. M. Bowden, and A. S. Manka, J. Appl. Phys. **83**, 2377 (1998).

[13] T. W. Ebbesen, H. J. Lezec, H. F. Ghaemi, T. Thio, and P. A. Wolff, Nature (London) **391**, 667 (1998).

[14] H. F. Ghaemi, T. Thio, D. E. Grupp, and T. W. Ebbesen, Phys. Rev. B **58**, 6779 (1998).

[15] T. J. Kim, T. Thio, T. W. Ebbesen, D. E. Grupp, and H. J. Lezec, Opt. Lett. **24**, 256 (1999).

[16] L. Martin-Moreno, F. J. Garcia-Vidal, H. J. Lezec, K. M. Pellerin, T. Thio, J. B. Pendry, and T. W. Ebbesen, Phys. Rev. Lett. **86**, 1114 (2001).

[17] F. I. Baida and D. V. Labeke, Phys. Rev. B **67**, 155314 (2003).

[18] J. A. Porto, F. J. Garcia-Vidal, and J. B. Pendry, Phys. Rev. Lett. **83**, 2845 (1999).

[19] F. Yang and J. R. Sambles, Phys. Rev. Lett. **89**, 063901 (2002).

[20] F. J. Garcia-Vidal, H. J. Lezec, T. W. Ebbesen, and L. Martin-Moreno, Phys. Rev. Lett. **90**, 213901 (2003).

[21] Q. Cao and P. Lalanne, Phys. Rev. Lett. **88**, 057403 (2002).

[22] M. M. J. Treacy, Phys. Rev. B **66**, 195105 (2002).

[23] Y. Takakura, Phys. Rev. Lett. **86**, 5601 (2001).

[24] W.-C. Tan, T. W. Preist, J. R. Sambles, M. B. Sobnack, and N. P. Wanstall, J. Opt. Soc. Am. A **15**, 2365 (1998).

[25] P. Lalanne, J. P. Hugonin, S. Astilean, M. Palamaru, and K. D. Möller, J. Opt. A, Pure Appl. Opt. **2**, 48 (2000).

[26] L. D. Landau and E. M. Lifshitz, *Electrodynamics of Continuous Media* (Pergamon, New York, 1960), Sec. 67.

[27] M. G. Salt, W. C. Tan, and W. L. Barnes, Appl. Phys. Lett. **77**, 193 (2000).